

# Nanoparticle-Cell Interactions Induced Apoptosis: A Case Study with Nanoconjugated Epidermal Growth Factor

*Ali Khanehzar,<sup>‡</sup> Juan C. Fraire,<sup>†,‡</sup> Min Xi,<sup>‡</sup> Amin Feizpour,<sup>‡</sup> Fangda Xu,<sup>‡</sup> Linxi Wu,<sup>‡</sup>*

*Eduardo A. Coronado<sup>†</sup> and Björn M. Reinhard<sup>‡,\*</sup>*

<sup>†</sup>INFIQC, Centro Laser de Ciencias Moleculares, Departamento de Físicoquímica, Facultad de Ciencias Químicas, Universidad Nacional de Córdoba, Córdoba 5000, Argentina.

<sup>‡</sup>Department of Chemistry and the Photonics Center, Boston University, Boston, Massachusetts 02215, United States.

\*E-mail: [bmr@bu.edu](mailto:bmr@bu.edu)

## **Supporting Information**

## Materials and Methods

### *Gold Nanosphere Synthesis.*

The synthesis of gold NP was performed using the Turkevich method.<sup>12</sup> For NP<sub>21.5</sub>, 1 mL of 0.2 wt% HAuCl<sub>4</sub> x H<sub>2</sub>O was diluted to 20 mL with Millipore water. The solution was boiled and 800  $\mu$ L 1 wt% sodium citrate tribasic dihydrate was injected under vigorous stirring and boiled for 30 min. Subsequently, the 20 nm colloid was diluted to 100 mL with deionized (DI) water. For NP<sub>40.4</sub>, 50 mL of 0.04 wt% HAuCl<sub>4</sub> xH<sub>2</sub>O and 50 mL of a 0.05 wt% ascorbic acid and 0.025 wt% sodium citrate tribasic dihydrate containing solution were added dropwise to the NP<sub>21.5</sub> seed solution. For NP<sub>78.9</sub>, 20 mL of NP<sub>40.4</sub> were diluted to 100 mL with Millipore water and the particles were grown to 80 nm by adding 50 mL of an aqueous 0.04 wt% HAuCl<sub>4</sub> xH<sub>2</sub>O solution and 50 mL of a 0.05 wt% ascorbic acid and 0.025 wt% sodium citrate tribasic dihydrate containing solution. In the last step of each procedure, the samples were boiled for 30 min. All NP concentrations used in this manuscript were quantified by UV-Vis using published extinction cross-sections (Ted Pella).

### *Gold NR Synthesis.*

Gold nanorods were synthesized using the seed-mediated growth technique described by Vigdeman *et al.*<sup>13</sup> In this technique, the first step is the generation of small NP employing a strong reducing agent such as sodium borohydride. In the second step, these seeds are added to a growth solution containing the metallic precursor together with a weaker reducing agent. Seed Synthesis: 460  $\mu$ L of a freshly prepared solution of 0.01 M sodium borohydride dissolved in 0.01 M sodium hydroxide were quickly injected into an HAuCl<sub>4</sub> solution (10 mL, 0.5 mM) containing 0.1 M CTAB under rapid stirring, leading to a change in color from greenish to light brown. Representative Synthesis of Nanorods: 70  $\mu$ L of a 0.1 M silver nitrate solution were added to a HAuCl<sub>4</sub> solution (10 mL, 0.5 mM) with 0.1 M CTAB, followed by addition of 500  $\mu$ L of a 0.1 M hydroquinone aqueous solution. The resulting mixture was stirred until it became clear. Finally,

160  $\mu$ L of seed solution were added, and the growth solution was mixed thoroughly and allowed to age overnight. Nanorods with different AR were obtained by varying the quantities of silver nitrate and seed added to the growth bath. NR concentrations were determined by UV-Vis spectroscopy assuming extinction cross-sections obtained from electromagnetic simulations with experimentally determined morphological parameters.

#### *EGF Quantification with ELISA.*

The number of EGF ligands bound per NP were determined by a human EGF ELISA kit (Life Technologies) following the manufacturer's protocol.

#### *Zeta-Potential Measurements.*

Zeta-potential measurements of CTAB stabilized NR and PEG-functionalized NP were performed on a Zetasizer Nano ZS90 (Malvern, Worcestershire, UK) at room temperature.

#### *Scanning Electron Microscopy.*

Scanning electron microscopy (SEM) images were obtained using a Zeiss Supra 55 VP scanning electron microscope with 10 kV EHT.

#### *Electromagnetic Calculations.*

The optical response of Au particles was computed using the Generalized Multiparticle Mie Theory (GMM) with the dielectric function by Palik.<sup>14</sup> For NR we used the approximation of prolate spheroidal particles, and the optical response was corrected according to the work of Kooij et al to account for the angular dependence of the extinction cross-section.<sup>15</sup>

#### *Cell Culture.*

MDA-MB-468 breast cancer cells were obtained from ATCC® (CRL-1555™) and maintained in DMEM with 10% fetal bovine serum, 100 units/mL of penicillin, 100  $\mu$ g/mL of streptomycin, and 2 mM of glutamine. Cells were grown in a 5% CO<sub>2</sub> containing atmosphere with 95% relative humidity in an incubator at 37 °C.

### *STAT3 Phosphorylation Measurements.*

NP<sub>78.9</sub>-EGF and NP<sub>40.4</sub>-EGF were incubated with cells at 37°C for 4 hrs. Cells were then detached and washed with 1x PBS. The cells were then lysed using the STAT3 (pY705) ELISA kit (abcam). The lysates were subsequently 5x diluted with 1x PBS and phosphorylation levels were quantified following the manufacturer's protocol.

### *Inhibition of Endocytosis.*

Clathrin-mediated uptake was inhibited by 30 min incubation of 500 µM Amantadine with cells.

Caveolae-mediated uptake was inhibited by 15 min incubation of 50 µg/mL nystatin with cells.

Pinocytosis was inhibited by incubation with 10 µg/mL colchicine for 0.5 h.

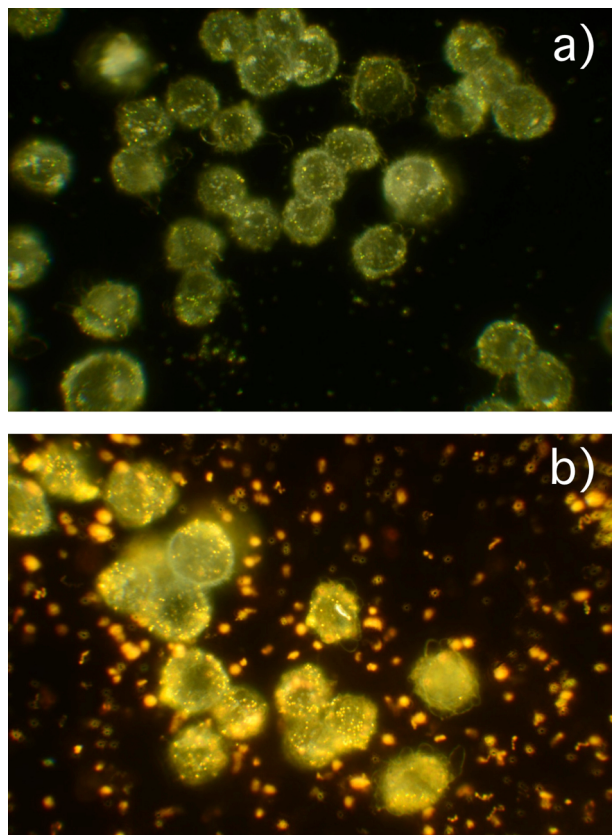


**Figure S1:** Darkfield images of MDA-MB-468 cells incubated with a) NP<sub>78.9</sub>-EGF and b) NP<sub>98.1</sub>-EGF particles for 20 min in DMEM at 37°C. The NP concentrations were 16 pM and 10 pM, respectively. Large metallic scatters on the substrate indicate NP agglomeration in b).

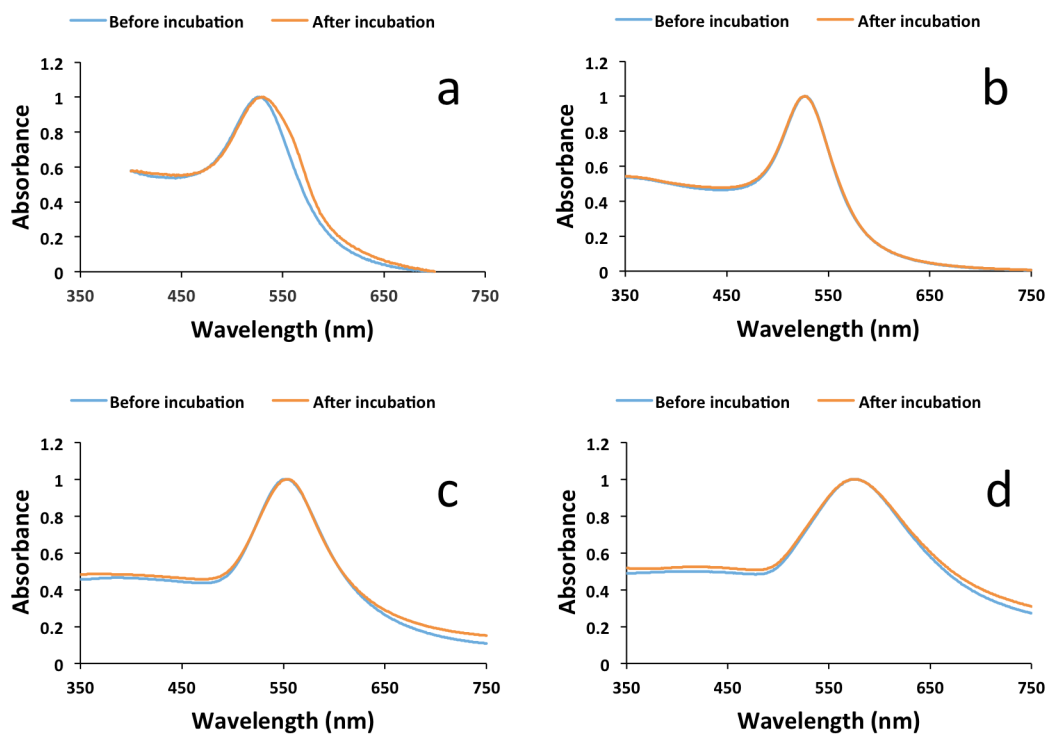


**Figure S2:** UV-Vis spectra of NP-EGF before (blue) and after (orange) incubation with MDA-MB-468 cells. The diameter of the NP cores is a)  $21.5 \pm 0.9$  nm, b)  $40.4 \pm 1.0$  nm, c)  $78.9 \pm 1.3$  nm, d)  $98.1 \pm 0.8$  nm. The UV-Vis spectra of the investigated metal NP are dominated by localized surface plasmon resonances (LSPRs), which red-shift upon NP agglomeration. For NP-EGF with average core diameter of  $> 21.5$  nm the spectra before and after incubation contain no indications of a systematic red-shift, confirming an excellent stability of these NP under the chosen experimental conditions. The NP<sub>21.5</sub>-EGF sample shows some asymmetric broadening on the long wavelength side indicative of some NP self-association.

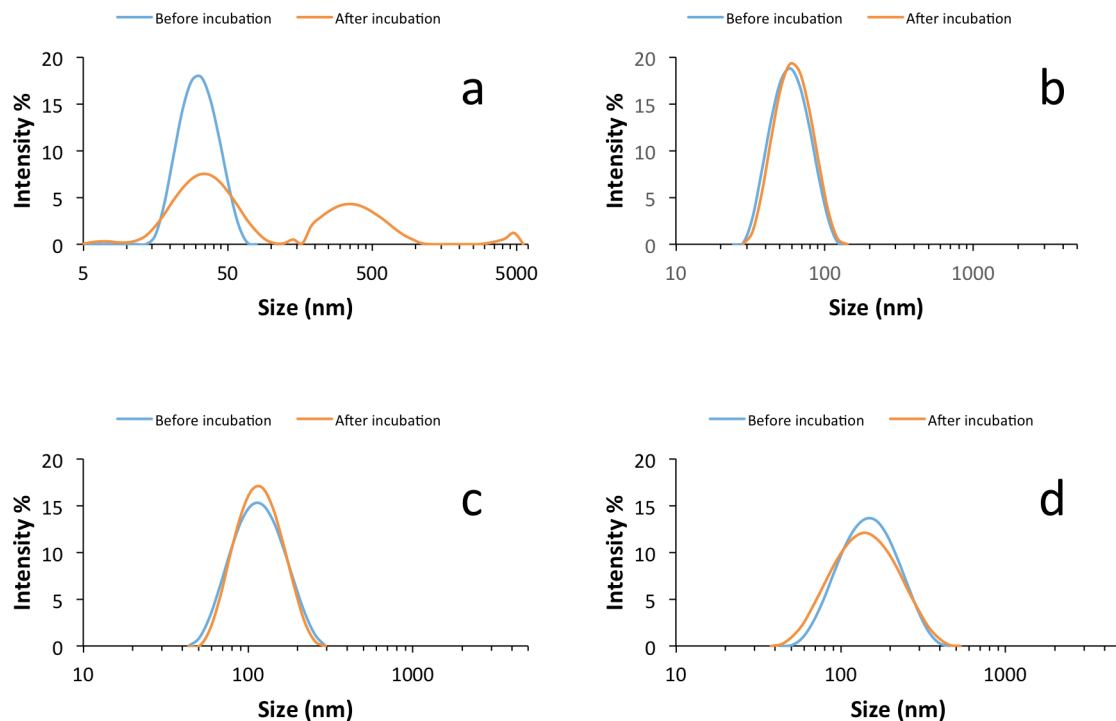


**Figure S3:** Hydrodynamic diameter distributions of NP-EGF before (blue) and after (orange) incubation with cells determined by DLS. Size of the NP core: a)  $21.5 \pm 0.9$  nm, b)  $40.4 \pm 1.0$  nm, c)  $78.9 \pm 1.3$  nm, d)  $98.1 \pm 0.8$  nm. All distributions are intensity statistics. All NP sizes show an increase in hydrodynamic diameter after functionalization with EGF, consistent with a high surface loading. The hydrodynamic diameters of NP-EGF with NP cores  $> 21.5$  nm show only small changes after incubation with the cells, confirming a high level of stability for the NP. Consistent with our interpretation of the broadened UV-Vis spectrum in Figure S2, for NP<sub>21.5</sub>-EGF the hydrodynamic size distribution shows three distinct peaks. The smallest corresponds to individual particles and the two larger peaks belong to agglomerates. If one considers the strong size dependence of the scattering signal on the particle size – in a first approximation as volume squared – it becomes, however, evident that the concentration of NP agglomerates is low. Based on the measured intensities, we estimate that the ratio of non-agglomerated / agglomerated NP is  $> 1E6$ .

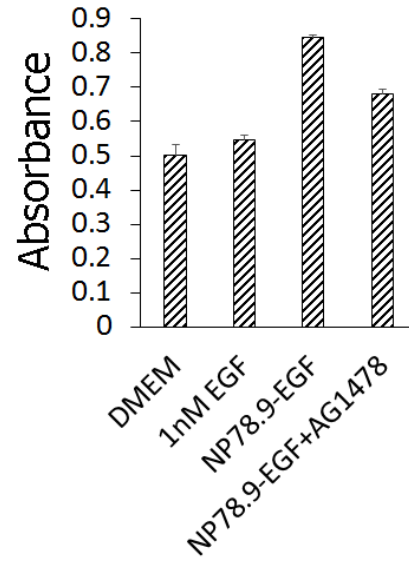


**Figure S4:** Phosphorylation levels for no treatment control, 1nM EGF, and NP<sub>78.9</sub>-EGF in the absence and presence of EGFR-selective RTK inhibitor (AG1478).



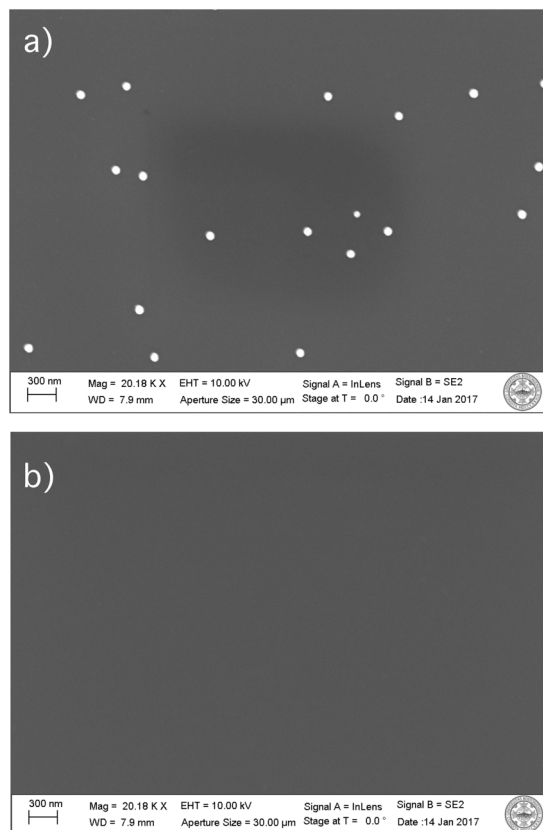


**Figure S5:** SEM images of NP<sub>78.9</sub>-EGF on silicon support a) without and b) with etching with KI/ I<sub>2</sub> etchant as described in the Materials and Methods section. The sample in a) was washed and treated identically as the sample in b), only the etchant was omitted. The removal of NP in b) confirms that the etchant completely removes all solvent-accessible gold NP under the chosen experimental conditions.

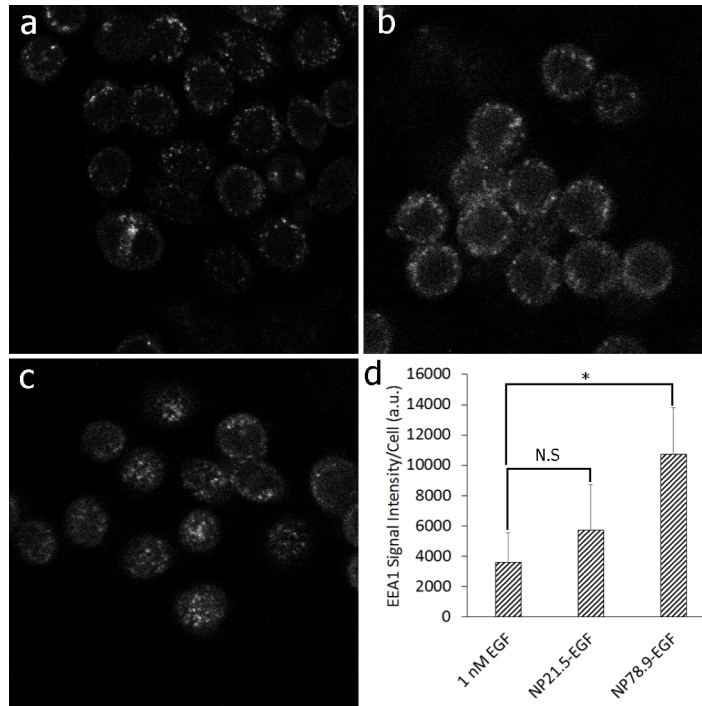


**Figure S6:** Confocal sections after immunolabeling of the early endosome marker EEA1 for a) 1 nM free EGF, b) 128 pM NP<sub>21.5</sub>-EGF, 8 pM NP<sub>78.9</sub>-EGF. The effective EGF concentration is 1 nM in a) – c). MDA-MB-468 cells were incubated with EGF or NP-EGF for 15 min. Then the buffer was exchanged and the cells were maintained for another 60 min in serum-free medium before the cells were fixed and EEA1 was stained following conventional immunolabeling protocols. For NP<sub>78.9</sub>-EGF in c) the EEA staining is less localized to the periphery than in a) and b). d) EEA signal intensity per cell determined from wide-field fluorescence images. Intensities were determined by i.) finding all labeled areas, ii.) multiplying these areas with their average intensities, and iii) summation of all signals. The analysis was performed with Image J. NS = not significant; \*p < 0.05. Data were collected from three independent experiments.

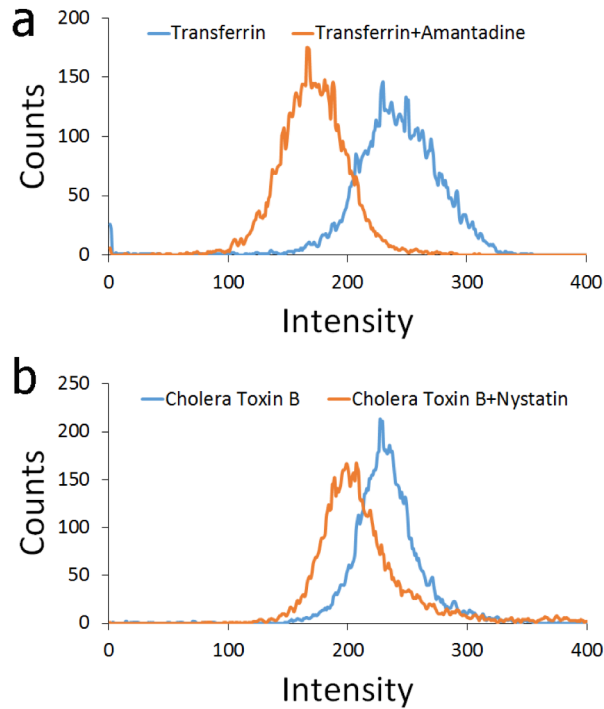


**Figure S7:** Fluorescence Intensity (flow cytometry) for MD-MBA-468 cells treated with fluorescently marked transferrin (positive control for clathrin mediated endocytosis) for 20 min and cholera toxin B (positive control for caveolae mediated endocytosis) for 20 min before and after treatment with a) amantadine for 30 min and b) nystatin for 15 min.

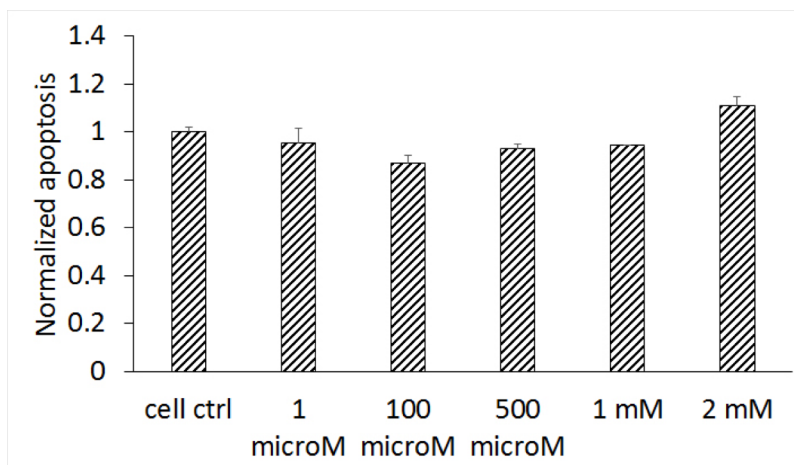


**Figure S8:** Apoptosis enhancement relative to the no treatment control for different trolox concentrations. Apoptosis was evaluated after 24 h.

**Table 1 | Physico-Chemical Characterization of NR used in Apoptosis Assays**

<b>Long Axis, <i>L</i> (nm)</b>	<b>Short Axis (nm)</b>	<b>Aspect Ratio</b>	<b>Maximum Extinction Wavelength (nm) (before PEGylation)</b>	<b>Maximum Extinction Wavelength (nm) (after PEGylation)</b>	<b>ζ-potential (mV) (before PEGylation)</b>	<b>ζ-potential (mV) (after PEGylation)</b>	<b>Volume (nm<sup>3</sup>)</b>	<b>Surface Area (nm<sup>2</sup>)</b>
45.8±5.5	18.2±1.3	2.5	526	522	27.8	-35.68	11915	3139
60.9±7.3	17.1±1.5	3.6	677	683	24.54	-40.87	13986	3730
71.6±9.6	13.3±1.5	5.4	907	932	20.30	-42.21	9722	3270
88.9±11.0	10.3±1.2	8.6	1108	1116	27.68	-39.81	7407	3044